Embedded QR code for part authentication in additive friction stir deposition

Tony Schmitz [a,b,*], Lino Costa [c], Brian K. Canfield [c], Joshua Kincaid [a], Ross Zameroski [a], Ryan Garcia [a], Curtis Frederick [d], Andres Marquez Rossy [b], Trevor M. Moeller [c]

[a] University of Tennessee, Knoxville, United States
[b] Oak Ridge National Laboratory, United States
[c] University of Tennessee Space Institute, United States
[d] ZEISS Industrial Quality Solutions, United States

ARTICLE INFO

ABSTRACT

This paper describes an approach for authentication of parts produced by additive friction stir deposition (AFSD) using an embedded QR tag. The manufacturing steps are: produce the QR tag by laser micromachining, deposit the base layers for the part using AFSD, machine a pocket in the top layer, insert the tag with the QR code(s) facing toward the printed material, and deposit the following layers over the QR tag to embed it within the part. Authentication is then provided using CT scanning to image the QR code at the known location within the AFSD part.

© 2022 Society of Manufacturing Engineers (SME). Published by Elsevier Ltd. All rights reserved.

1. Introduction

Authentication for computer access is ubiquitous, such as two-factor authentication for securing online accounts. This requirement also extends to manufactured parts. As an example, multiple efforts have been completed for fiber reinforced composite parts due to the potential for malicious process modification or substandard materials. Approaches have included inserted radio frequency identification (RFID) tags [1–2], magnetic inks [3–5], dyes [6–7], quantum dots [8], and nanoparticles [9]. QR codes has also been printed on the surface of polymer parts produced by fused filament fabrication (FFF) and inkjet printing [10–11]. Concerns also exist for counterfeiting or modification of metal parts, particularly for defense and human safety applications. Security and tracking using selective laser sintering (SLS) to print QR codes [12] and surface application of photoluminescent micropatterned tags have been studied, for example [13]. In this work we demonstrate embedding a QR code within an aluminum coupon fabricated using additive friction stir deposition (AFSD). Prior efforts have demonstrated

the validity of AFSD for metal part fabrication [14–17, for example].

2. Materials and methods

The approach followed in this study was to laser micromachine QR codes on the surface of an aluminum tag. This tag was then embedded in an AFSD part by: 1) depositing several layers of 6061 aluminum; 2) machining a pocket in the top layer; 3) inserting the tag in the pocket with the QR code facing toward the pocket bottom; and 4) depositing additional layers over the tag using AFSD. To confirm the results, both optical microscopy and computed tomography (CT) were applied. The procedure is described in the following sections.

2.1. Micromachining

Six QR code patterns covering a range of sizes were machined on a 25 mm × 50 mm × 2 mm 6061-T6 aluminum tag that was pre-sanded using 1200 grit SiC paper to provide a smooth working surface with randomized residual scratch/dig features; see Fig. 1, where the dimensions were obtained with an Alicona InfiniteFocusSL 3D measuring system. The tag was seated and leveled on a positioning stage with 50 mm travel in both transverse axes (X

---

* Corresponding author at: University of Tennessee, Knoxville, 114 Perkins Hall, Knoxville, TN 37902, United States.
E-mail address: tony.schmitz@utk.edu (T. Schmitz).
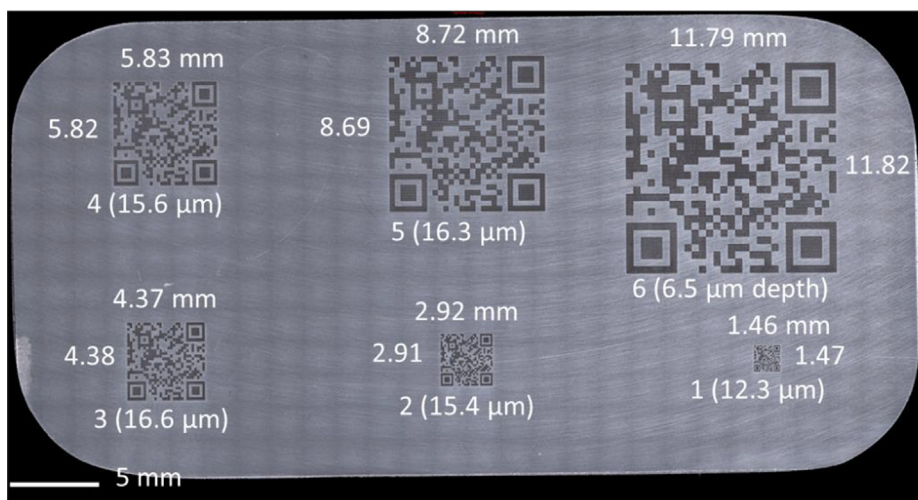
Fig. 1. Digital microscope image of six QR codes (labeled 1–6, smallest to largest) and dimensions, including width (mm), height (mm), and depth (μm). Each code is the same, but the scale changes.

and Y) and 3 mm travel in the axial direction (Z). A.png file containing the QR code was read into a custom National Instruments LabVIEW Virtual Instrument and converted into scalable travel-point coordinates. A pulsed, ultrafast IR laser beam (Amplitude Systèmes Tangerine, 1030 nm, 8 ps, 7 μJ, 100 kHz) was focused at the tag surface by a 32x microscope objective (Leitz Wetzlar, 0.60NA). The tag was translated along an alternating X-Y raster path at 10 mm/s to ablate each QR code. A nitrogen stream was directed over the work area to clear material and protect the objective from contamination. To achieve a suitable ablation depth, each pattern was swabbed with acetone-soaked lens tissue after the first pass to clear debris and was then exposed a second time, yielding approximately 15 μm deep features. However, during cleaning of code 6 (Fig. 1), the tag was accidently shifted, so a second pass over this pattern was not completed, leaving it shallower than the other five. Following laser micromachining, the tag was sonicated in acetone for 1 min.

2.2. First AFSD

The first AFSD process was completed using a MELD Manufacturing L3 machine, where wrought stock (9.53 mm square × 508 mm long) is forced axially through a rotating spindle against a build plate (or prior print layer). The frictional heating and subsequent plastic deformation provided heat to soften the material and enable layer-by-layer deposition without melting. In this step, material was deposited in 11 layers that were 2.5 mm thick × 52 mm wide using a spindle speed of 350 rpm[1], stock feed rate of 152 mm/min through the spindle, and traverse feed rate of 102 mm/min for the rotating tool relative to the 6061-T6 aluminum build plate.

2.3. First machining

After AFSD, a 26.2 mm × 51.6 mm × 3.2 mm pocket was machined in the top layer of the printed aluminum. The dimensions were selected based on the micromachined QR tag (Section 2.1). To connect the AFSD and machining coordinate

systems, the AFSD part and build plate were measured by structured light scanning (GOM ATOS Q). The subsequent 3D mesh was imported into the computer-aided manufacturing (CAM) software as the stock model, where the measurement origin was selected to be the build plate's top corner; see Fig. 2. The tool paths were then generated in this coordinate system. When the part was placed in the Haas VF-4 computer numerical control (CNC) milling machine, on-machine probing was used to locate the build plate corner and transfer the coordinate system origin [18]. Orientation was ensured by clamping the build plate in a pre-aligned vise. While a preferred solution may be to deposit and machine using the same system, the MELD Manufacturing L3 does not have a milling spindle; the tool-spindle connection is not compatible with traditional milling spindle-holder connections (such as CAT-40 or HSK-63A).

After machining, the pocket was measured using a coordinate measuring machine to identify its location relative to the build plate; the measurement origin was again selected to be the build plate's top corner for the Section 2.5 s machining step after material was printed over the QR tag. Prior to the second printing step (Section 2.4), the QR tag was inserted in the machined pocket with the QR code facing the pocket bottom away from the second AFSD step.

2.4. Second AFSD

After the QR tag was inserted in the pocket, three new layers were deposited over the top of the pocket and first 11 layers. The QR tag was then embedded within the aluminum part and not visible from the outside; see Fig. 2.

2.5. Second machining

To enable convenient manipulation for follow-on CT scanning, a coupon was machined from the AFSD part, where the coupon dimensions were selected to be 3 mm larger in each Cartesian direction than the original QR tag that was embedded in the AFSD part. Using the build plate origin as a reference, the coupon was released by milling away the surrounding material, where the tool paths were generated using the pocket location identified by the CMM in Section 2.3. The complete manufacturing sequence is displayed in Fig. 2.

---

[1] The spindle speed was reduced layer-by-layer as more process heat was retained in the part. The starting spindle speed was 350 rpm and the final spindle speed was 200 rpm.

Fig. 2. Manufacturing sequence for embedding QR tag (clockwise from top left). (Top left) The AFSD part was scanned to identify the stock model for the first machining operation. (Top right) The top surface was faced and the pocket was machined to hold the QR tag. (Bottom right) Additional layers were deposited over the QR tag. (Bottom left) A coupon was obtained for CT scanning by machining material away with a 3 mm perimeter around the embedded QR tag.
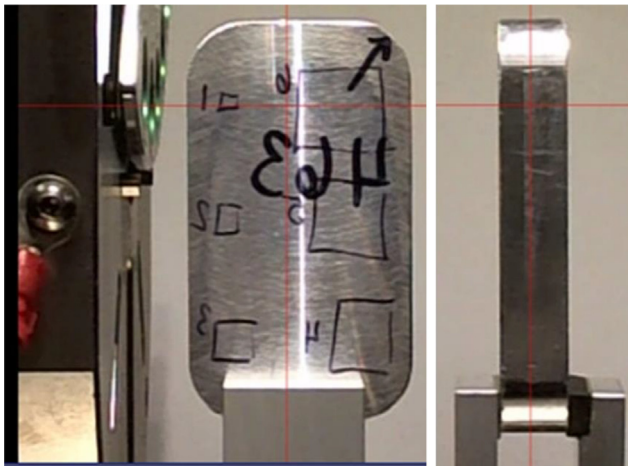
Fig. 3. ZEISS VERSA 620 setup. (Left) 90 deg orientation. (Right) 0 deg orientation.

3. Results

CT scans were completed for the aluminum coupon with the embedded QR tag. The scans were completed using a ZEISS VERSA 620 with a voxel size of 18 μm. The setup is displayed in Fig. 3 and an example scan is provided in Fig. 4. For the selected field of view, codes 6 and 1 are observed. With the 18 μm voxel size, more detail is seen for the larger code 6 (11.8 mm square). The intent for the embedded tag is that the CT image can ultimately be scanned with a smart phone or similar device to confirm the part's authenticity. Additional research will fully enable this capability.

4. Conclusions

This paper provided a proof of concept for authentication of parts produced by additive friction stir deposition (AFSD) using an embedded QR tag and CT scanning. The selected approach included laser micromachining to write the QR codes on the surface of an aluminum tag. After depositing several layers using AFSD, the process was paused and a pocket was machined in the top layer to accept the tag. The QR codes were oriented so that the micromachined surface faced away from the next printing layer so that the severe plastic deformation caused by AFSD did not disturb the QR codes. After depositing additional layers over the pocket, the QR tag was embedded in the print in a known location. Subsequent CT scanning showed that the QR codes were vis-
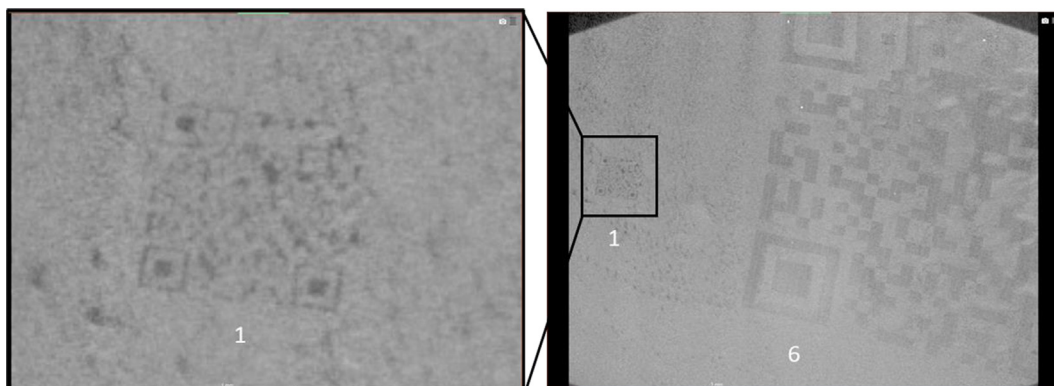
Fig. 4. CT scan of embedded QR tag. In the image field of view, codes 1 and 6 are observed. The left inset shows code 1 only.

ible. Future efforts will advance this initial study to refine the laser micromachined QR code scale and depth and confirm that the CT image can obtained with adequate resolution and accuracy to authenticate the part using a smart phone (or similar device) scan of the QR code. Application of this approach will be best suited to high value components that warrant the cost and availability of a CT scanner.

Declaration of Competing Interest

The authors declare that they have no known competing financial interests or personal relationships that could have appeared to influence the work reported in this paper.

Acknowledgements

References

[1] Bauchot F, Clement J-Y, Marmigere G, Second P. Chipless RFID tag and method for communicating with the RFID tag. US8068010B2; 2011.
[2] Burkholder RJ, Kiourti A, Shao S, Volakis JL. RFID tag. USD763833S1; 2016.
[3] Kokkinis D, Schaffner M, Studart AR. Multimaterial magnetically assisted 3D printing of composite materials. Nat Commun 2015;6(1):1–10.
[4] Herbert WG, Maier GJ. Magnetic ink composition, magnetic ink character recognition process, and magnetically readable structures. EP2390292B1 2013.
[5] Saleh E, Woolliams P, Clarke B, Gregory A, Greedy S, Smartt C, et al. 3D inkjet-printed UV-curable inks for multi-functional electromagnetic applications. Addit Manuf 2017;13:143–8.
[6] Tang L, Whalen J, Schutte G, Weder C. Stimuli-responsive epoxy coatings. ACS Appl Mater Interfaces 2009;1(3):688–96.
[7] McFadden PD, Frederick K, Argüello LA, Zhang Y, Vandiver P, Odegaard N, et al. UV fluorescent epoxy adhesives from noncovalent and covalent incorporation of coumarin dyes. ACS Appl Mater Interfaces 2017;9(11):10061–8.
[8] Zou W, Du ZJ, Li HQ, Zhang C. A transparent and luminescent epoxy nanocomposite containing CdSe QDs with amido group-functionalized ligands. J Mater Chem 2011;21(35):13276–82.
[9] Pansare AV, Khairkar SR, Shedge AA, Chhatre SY, Patil VR, Nagarkar AA. In situ nanoparticle embedding for authentication of epoxy composites. Adv Mater 2018;30(33):1801523.
[10] Gültekin S, Ural A, Yaman U. Embedding QR codes on the interior surfaces of FFF fabricated parts. Proc Manuf 2019;39:519–25.
[11] Kikuchi R, Yoshikawa S, Jayaraman PK, Zheng J, Maekawa T. Embedding QR codes onto B-spline surfaces for 3D printing. Comput Aided Des 2018;102:215–23.
[12] Chen F, Luo Y, Tsoutsos NG, Maniatakos M, Shahin K, Gupta N. Embedding tracking codes in additive manufactured parts for product authentication. Adv Eng Mater 2019;21(4):1800495.
[13] Platel R, Palleau E, Vaure L, Raffy S, Guerin F, Nayral C, et al. Micropatterning of Adhesive Epoxy with Embedded Colloidal Quantum Dots for Authentication and Tracing. ACS Appl Nano Mater 2021;4(4):3537–44.
[14] Hang ZY, Jones ME, Brady GW, Griffiths RJ, Garcia D, Rauch HA, et al. Non-beam-based metal additive manufacturing enabled by additive friction stir deposition. Scripta Comput Sci Appl Math Comput Sci Appl Math Materialia 2018;153:122–30.
[15] Khodabakhshi F, Gerlich AP. Potentials and strategies of solid-state additive friction-stir manufacturing technology: A critical review. J Manuf Process 2018;36:77–92.
[16] Yu HZ, Mishra RS. Additive friction stir deposition: a deformation processing route to metal additive manufacturing. Mater Res Lett 2021;9(2):71–83.
[17] Gopan V, Wins KLD, Surendran A. Innovative potential of additive friction stir deposition among current laser based metal additive manufacturing processes: A review. CIRP J Manuf Sci Technol 2021;32:228–48.
[18] Cornelius A, Dvorak J, Jacobs L, Penney J, Schmitz T. Combination of structured light scanning and external fiducials for coordinate system transfer in hybrid manufacturing. J Manuf Process 2021;68:1824–36.